

**This item is the archived peer-reviewed author-version of:**

Tailoring the functional properties of polyurethane foam with dispersions of carbon nanofiber for power generator applications

**Reference:**

Sathiyamoorthy Suhasini, Girijakumari Greeshma, Kannan Prashant, Venugopal Kathirvel, Thiruvottriyur Shanmugam Saranya, Veluswamy Pandiyarasan, De Wael Karolien, Ikeda Hiroya.- Tailoring the functional properties of polyurethane foam with dispersions of carbon nanofiber for power generator applications  
Applied surface science - ISSN 0169-4332 - Amsterdam, Elsevier science bv, 449(2018), p. 507-513  
Full text (Publisher's DOI): <https://doi.org/10.1016/J.APSUSC.2018.01.088>  
To cite this reference: <https://hdl.handle.net/10067/1512870151162165141>

**Tailoring the functional properties of polyurethane foam with dispersions of carbon nanofiber for power generator applications**

Suhasini Sathiyamoorthy<sup>1</sup>, Greeshma Girijakumrai<sup>2</sup>, Prashanth Kannan<sup>2</sup>, Kathirvel Venugopal<sup>2#</sup>, Saranya Thiruvottriyur Shanmugam<sup>3#</sup>, Pandiyarasan Veluswamy<sup>4,5\*</sup>, Karolien De Wael<sup>3</sup>, Hiroya Ikeda<sup>4</sup>

<sup>1</sup>Department of Electronics and Communication Engineering, SRM University,  
Chennai, India – 603203

<sup>2</sup>Department of Physics and Nanotechnology, SRM University, Kattankulathur, India-603203.

<sup>3</sup>University of Antwerp, Faculty of Sciences, Department of Chemistry, AXES Research Group,  
Groenenborgerlaan 171, 2020 Antwerp, Belgium

<sup>4</sup>Research Institute of Electronics, Shizuoka University, Hamamatsu, Japan -4328018.

<sup>5</sup>Engineering Research Center (ERC) for Flexible Thermoelectric Device Technology, Daejeon  
34141, Republic of Korea.

\*Corresponding author Email:

pandiyarasan@yahoo.co.in (Dr. PV)

#Co-Corresponding author Email:

sarashanmugam@gmail.com (Mrs. STS)

kathir.phy@gmail.com (Dr. KP)

**Abstract:**

To produce effective thermoelectric nanocomposite with carbon nanofibers (CNF) incorporated polyurethane (PU) foams are prepared via in-situ polymerization method to create a synergy that would produce a high thermopower. The formation mechanism of foams, the reaction kinetics, and the physical properties such as density and water absorption are studied before and after CNF incorporation. The microscopy images showed a uniform dispersion of CNF in the PU matrix of the prepared foams. Spectroscopic studies such as X-ray photoelectron and laser Raman spectroscopy suggested the existence of a tight intermolecular binding interaction between the carbon nanofibers and the PU matrix in the prepared composite foams. It found that the thermopower is directly dependent on the concentration of carbon nanofiber since, with rising concentration of 1% to 3%, the coefficient increased from 1.2  $\mu\text{V/K}$  to 11.9  $\mu\text{V/K}$  respectively, a value larger than that reported for PU foams. This unique nanocomposite offers a new opportunity to recycle waste heat in portable/ wearable electronics and other applications which will broaden the development of low weight, and mechanical flexibility.

**Keywords:**

Nanocomposites; Organic compounds; Chemical synthesis; Raman spectroscopy; Surface properties; Thermopower.

## 1. Introduction

Polymer nanocomposites as a class of materials have attracted much attention in this decade. Owing to their exceptional properties such as thermal stability, mechanical stability, conductivity, gas barrier performance, applications in flexible electronic devices, etc.<sup>1-4</sup> These improved properties of polymer nanocomposites arise due to the presence of nanosize filler in the organic polymer matrix.<sup>5</sup> Recently, a significant highly polymer electronic devices is one of the most interesting industrial technology.<sup>6</sup> Hence, there is, now, an emphasis on continuous research towards advanced polymeric materials with improved properties.<sup>7</sup>

Initially, the blending of different classes of polymers was used as a method to fabricate new materials with unique properties.<sup>8</sup> However, blending led to only a marginal improvement in the physical properties which were still inadequate for engineering applications.<sup>9</sup> Then, to improve the strength and stiffness of the polymer materials, different kinds of organic and inorganic fillers were used. To the dispersion of a few inorganic materials such as metal nanoparticles, metal oxides (MgO, ZrO<sub>2</sub>), carbon materials (carbon nanotubes (CNT), carbon nanofibres (CNF), graphene) and clays into the polymer matrix. Significantly improve the performance of the polymer materials due to the extraordinary properties they impart, which include electric, magnetic, mechanical, thermal, optical, chemical, and other such stimulation.<sup>10-14</sup> Moreover, they designed in almost any conceivable shape, and their properties can be tailored to suit many diverse applications.

Recently, flexible/ portable electronics emerged as a new class of electronic device for energy production (piezoelectric, thermoelectric) and energy storage (batteries and supercapacitors) devices.<sup>15,16</sup> Polymers are an ideal choice for the fabrication of such high

performance flexible electronic devices.<sup>17</sup> In this regard, thermoelectric energy harvesting is the most promising energy harvesting technique in which an electrical output achieved via a difference in temperature.<sup>18</sup> Several conducting polymers such as polyaniline, polypyrrole, poly(3,4-ethylenedioxythiophene) have shown excellent thermoelectric properties.<sup>19-21</sup> Polyurethane is a polymer formed via the reaction between polyisocyanates with polyols and possess excellent thermal insulation properties.<sup>22</sup>

The most common method of producing PU foams is via polymerization reaction of a polyol with an isocyanate, resulting in a three-dimensional cross-linked polymeric structure.<sup>23</sup> Depending on the proportions of the polyol blend with the isocyanate, the properties and consequently, the nature of polymers differ.<sup>24</sup> Lower amounts of polyol result in rigid polymers, whereas increasing the polyol content makes the foams flexible. For the formation of foam with well-defined cell structures, a blowing agent with a low boiling point is needed to cause the foam to rise. The blowing agent gets trapped under the polymer structure as it evaporates due to the heat of reaction.<sup>25</sup> It has intrinsically low thermal conductivities with low density and weight, making them prime candidates for competitive thermal barriers.<sup>26</sup>

As an excellent alternative candidate to improve the properties of PU foam, several researchers have attempted the dispersion of nanoscaled fillers such as titanium oxide, silica, nanoclays, graphene, carbon nanotubes to induce changes in the polymer matrix by interface interaction.<sup>27-29</sup> It has spurred the interest in developing nanocomposite foams with an aim to reduce the density while maintaining or improving their properties. Among the various fillers, carbon nanofiber is attractive due to its fibre morphology which can result in high surface–interface reaction with the polymer matrix, thereby resulting in improved thermopower properties and decrease the thermal conductivity.<sup>30</sup> The functionalized carbon nanofiber showed excellent

dispersion and stability in water without any dispersion agent. Reported here is a polyurethane polymer foam dispersion with carbon nanofiber enhanced material properties such as compressive strength, water absorption, density and a room temperature resultant thermoelectric properties.

## **2. Experimental**

### ***2.1 Materials***

Polyether (glycol based polyol) of density 1.1 g/cc and viscosity 9000 cps obtained from Sigma Aldrich. DABCO-TMR4 and DBTDL purchased from Air Products. Rubinate M, the isocyanate is purchased from Huntsman Corporation, India. Applied Science Inc supplied vapour grown Carbon nanofiber. TEGOSTAB B8408, chlorodifluoromethane (HCFC) and polymethylene polyphenyl polyisocyanate (PMDI) obtained from Sigma Aldrich.

### ***2.2 Preparation of polyurethane foam***

The polyurethane foam prepared by the in-situ polymerization route as reported in the literature.<sup>31</sup> The polyurethane foam was synthesized by ratios mentioned in Table 1 but without nanofiller. There are two different solutions that have been made, one is as mentioned table 1 without nanofiller and another one is PMDI solution. The table 1 solution taken as stoichiometric ratio 1 and PMDI took as stoichiometric ratio 2. Both were mixed well using the ultra-sonication method with different time intervals of 15 min, 30 min, 45 min, and 60 min. Then the blowing agent HCFC is added in the range of 40 ml per 100 g of above solution and mixed thoroughly with a mechanical stirrer. After 6 s of stirring, the mixture is removed and poured into a paper mould of dimension 25 cm X 25 cm X 7 cm and left to rise by the free-rise process. The reaction kinetics noted with the help of a stopwatch, and the foam is left to cure in a sealed room for 24 h before being de-moulded.

### ***2.3 Preparation of CNF/polyurethane foam***

CNF was carefully dried at 60°C for 24 h in a vacuum oven to prevent any contamination. The CNF, taken as 1% and 3 % concentrations and mixed with first part of the solution as mentioned in table 1. Now the CNF would act as nanofillers and is dispersed in the polyol blend matrix using ultrasonication with time intervals of 15 min, 30 min, 45 min and 60 min for both 1 % and 3 % of CNF concentrations. Once the sonication is done, the second solution (PMDI) added to the polyol blend solution, but mechanical stirrer is not used to avoid CNF agglomerate. Figure 1 elaborates the steps involved in the polyol blend-CNF fabrication process.

**Table 1:** Formulation of polyol blend

Component	Ratio (%)
Polyester	93.6
DABCO TMR4	2.246
DBTDL	0.22
KOSMOS 75	1.49
TEGO B8408	1.83
Water	0.6

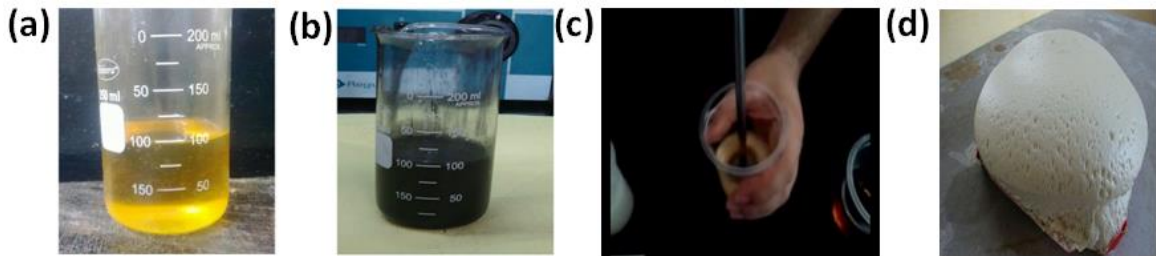


*Fig. 1 Preparation of CNF-incorporated polyurethane foams*

## 2.4 Characterizations

XRD analysis was performed using an X-ray diffractometer system (X'pert PRO PANalytical Instrument) at a scanning rate of  $2\theta$  ranging from  $10^\circ$  to  $70^\circ$  using Cu  $K\alpha$  radiation of  $0.02^\circ/s$  step interval ( $\lambda=0.154$  nm). Raman spectra (JASCO NRS -7100, Japan) of the foam (bare and CNF) were studied, with an operation at 11.8 mW laser power and an excitation wavelength of 532.1 nm with an argon-ion laser. The field emission scanning microscopy (FESEM; JEOL JSM 7001F) revealed that the morphology of the as obtained bare foam and CNF foam. A small amount of gold was sputter coated onto the surface of all the fabric specimens to get clear micrographs. To determine the steady-state heat transfer properties, thermal conductivity, and thermal resistance, Guarded Hot Plate Apparatus used. Flat slab specimens prepared by the International standards of ISO 8302, and ASTM C-177. The Seebeck coefficient was measured by the same method as that used in our previous studies.<sup>32</sup> The thermoelectromotive force (TEMF) measured by using two probes that were attached to the sample surface. Thus, the Seebeck coefficient was determined using the equation,  $S = -\Delta V/\Delta T$ , where  $\Delta V \equiv V_{TH} - V_{TL} \equiv TEMF$  and  $\Delta T \equiv T_H - T_L$ . Here,  $V_{TH}$  and  $V_{TL}$  are the potentials at the high-temperature side  $T_H$  and the low-temperature side  $T_L$  respectively.

### **3. Results and discussions**

#### ***3.1 Properties of CNF nanofiller***

The CNF nanofillers used in this study obtained from Applied Science Inc. and their corresponding FESEM, XPS, and Raman analysis provided in the Fig. 4. The FESEM micrograph (as shown in Fig. 4(a)) shows the presence of fibre morphology in the obtained CNF with diameters of about 100-150 nm and length about 50 -100  $\mu\text{m}$ , respectively. The XPS deconvoluted spectrum (Fig. 4(b)) shows the presence of C-C components at 284.5 eV respectively, which is in close agreement



with the previous reports on the CNF.<sup>33</sup> The Raman spectrum (Fig. 4(c)) of the CNF shows the presence of G and D bands, located at 1575 and 1350  $\text{cm}^{-1}$ , respectively.<sup>34</sup> The observed results are in close agreement with the previous work on the carbon nanofibers.

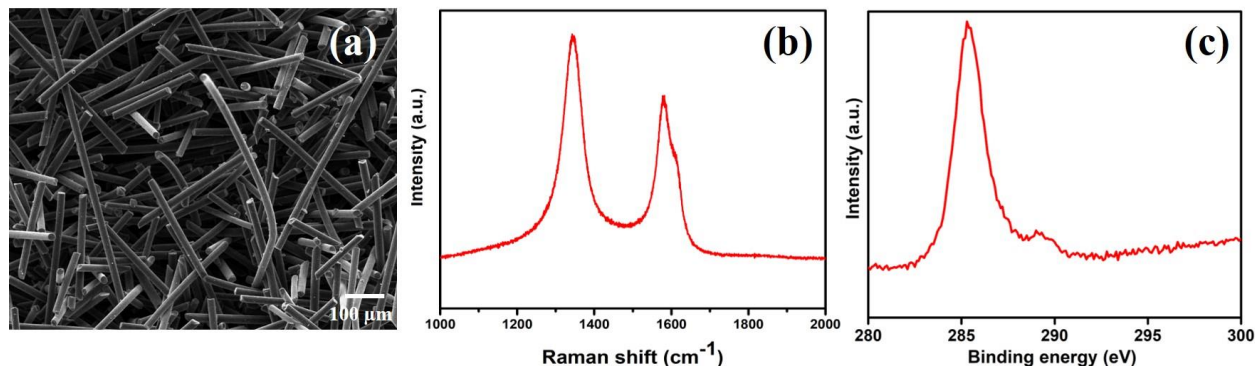


Fig. 2. Scanning electron microscope (a), laser Raman spectrum (b), and X-ray photoelectron spectrum (c) of carbon nanofibers.

### 3.2 Properties of CNF nanofiller in the polymer matrix

This CNF used as a conductive additive in the polyurethane foams and its physio-mechanical properties shown in Fig. 4. The CNF impregnated polyurethane foams prepared by the *in-situ* polymerization route (similar to the method of preparation of bare polyurethane foams) and the reaction kinetics as well as the physical and mechanical properties of the prepared foam are analyzed.<sup>35</sup> In general, the polymerization of polyurethane foam can be monitored by the specific time markers such as cream time, rise time, and tack free time intervals, during the reaction between polyol matrix and the curing agent. The observed cream time, rise time and tack free time, for the bare polyurethane foams are measured to be 14, 56, and 59 minutes, respectively. There are some significant changes observed in the reaction kinetics due to the impregnation of CNF in the PU foams. As shown in Fig.3 the observed cream time, rise time and tack free times for the CNF (1%) impregnated polyurethane foams are 13, 54, and 56, min respectively and these times are about 13, 52, and 54 for the CNF (3%)-PU foams. It shows that the presence of CNF leads to

faster reaction kinetics, that is, a faster reaction mechanism compared to that of the bare PU. This study substantiates that the addition of CNF provides more active sites in the PU matrix and hence, catalysis the polymerization reaction.

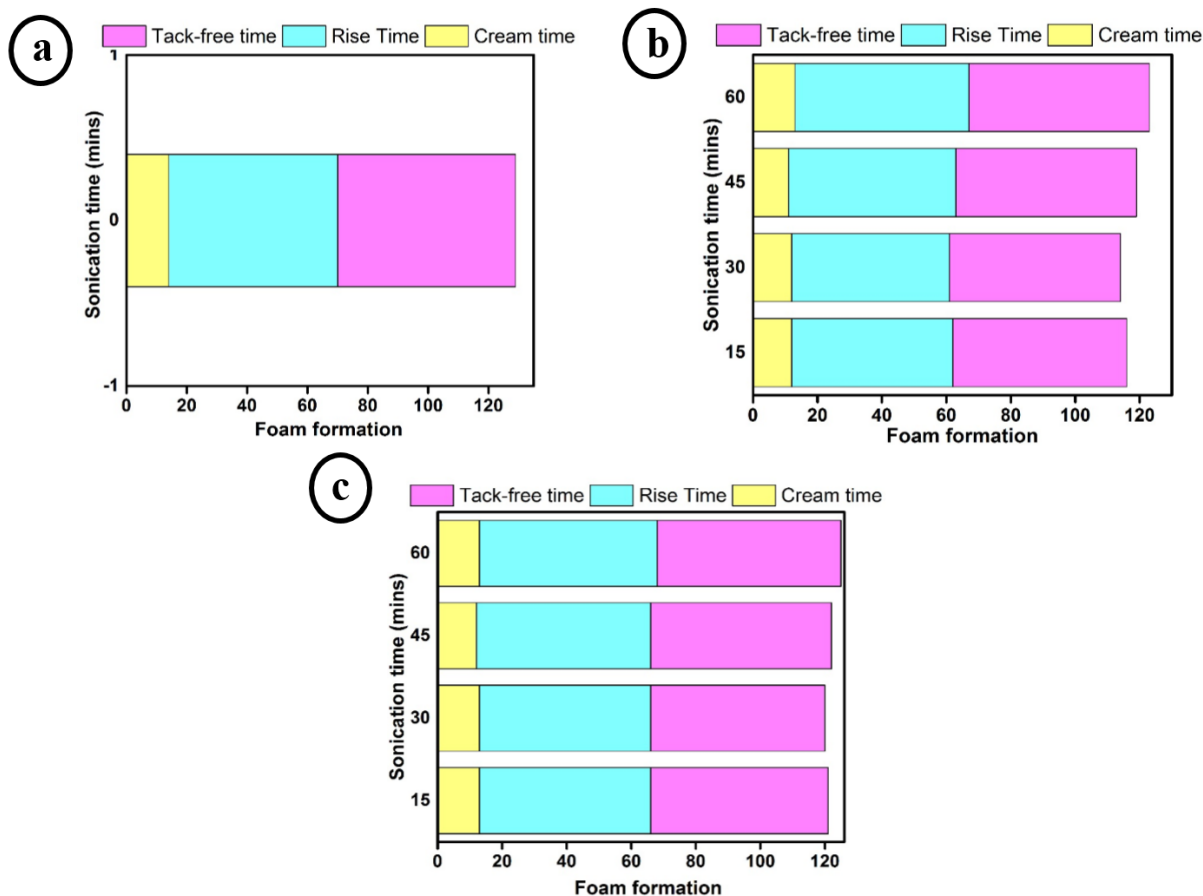


Fig. 3 a) PU foam, b) PU blend 1% CNF foam and c) PU blend 3% CNF foam

The density measurements noted by preparing cubic blocks of size 50 mm x 50 mm x 50 mm out of the cured foam, measuring the weight under a conventional weight balance and calculating the density as a function of mass over. It shows a clear correlation between the density and time of mixing and the CNF cause an alternating effect on density with increasing sonication time. The density of the bare PU foam, CNF (1%) PU-foam and CNF (3%)-PU foam calculated as 22.6, 24.01, and 25.68, kg/m<sup>3</sup>, suggesting the role of CNF in the improved density of the PU foams as

shown in Fig. 4 (a). It shows a clear correlation between the density and time of mixing and the CNF cause an alternating effect on density with increasing sonication time.

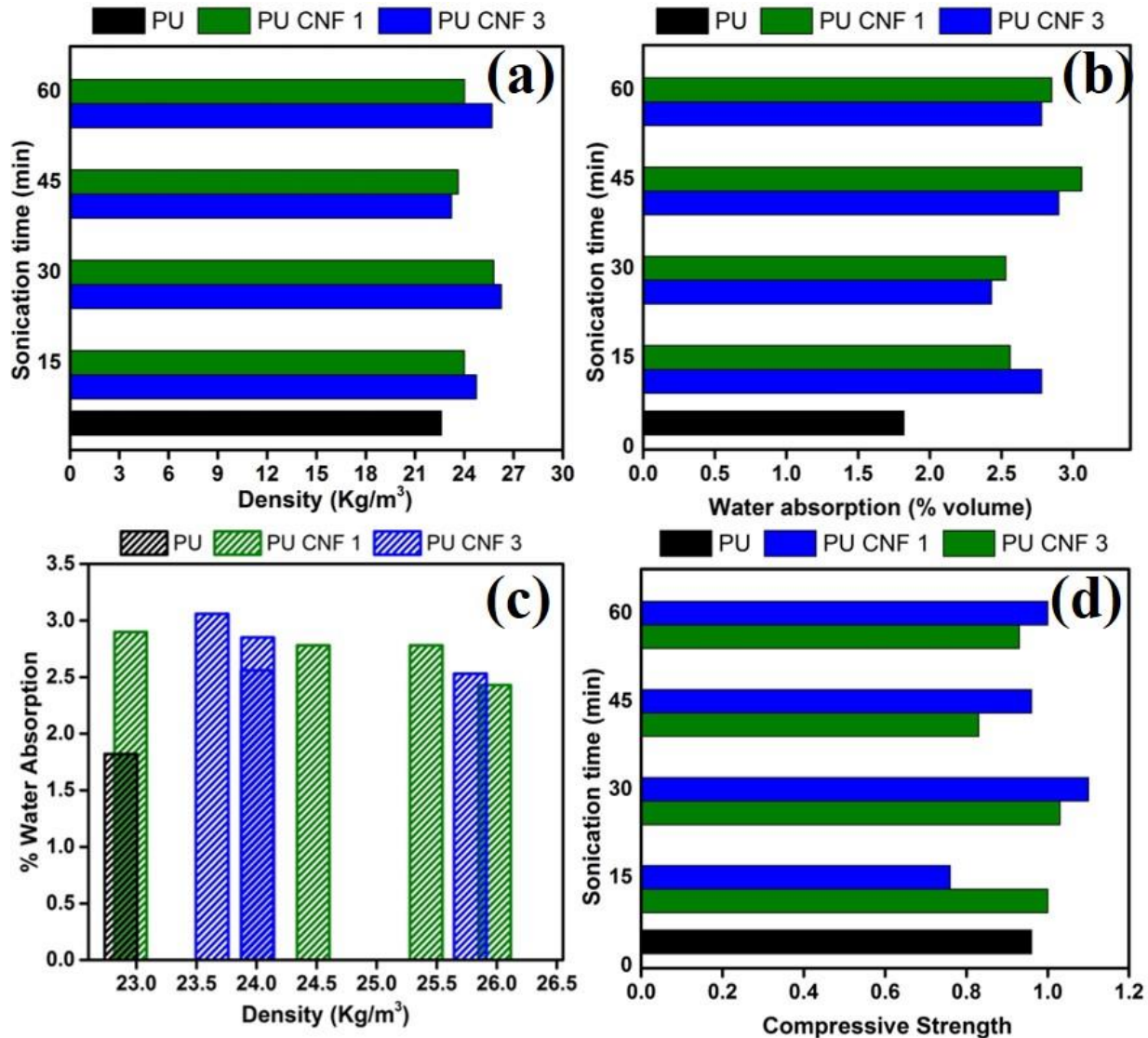
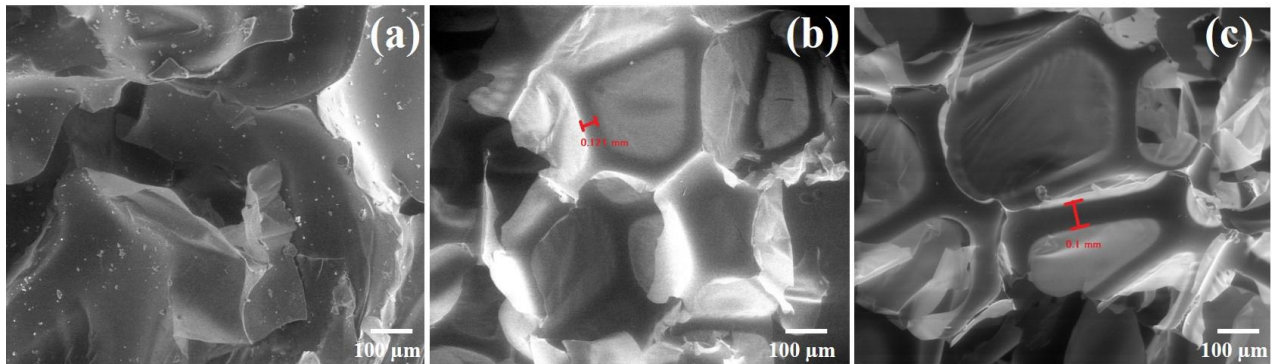


Fig. 4 Physio-Mechanical properties of PU-CNF foam

The water absorption properties of the prepared foams were measured by completely immersing the foam blocks in water for sets of 24 h, 48 h, and 72 h and then, measuring the initial and final weights, before and after soaking. The difference in weight over the volume is taken as the volume percent water absorption. The maximum permissible value is taken to be not above 3%. The study suggested the presence of CNF results in improved water absorption on its surfaces. The water

absorption values of the bare PU foam, CNF (1%) PU-foam and CNF (3%)-PU foam are observed to be about 1.82, 2.78, and 2.85 % respectively as shown in Fig. (b) and (c). The studies highlight that the inclusion of CNF modified the properties of the PU foam. Since the foams are not much use as peening load-bearing materials, but sometimes it required that they can handle minor loads during the fabrication process and shear forces. The foam blocks noted in the direction of rising and force is applied on each side with equal intensity until compressive yield obtained. The Fig. 4 (d) follow the same pattern as the density indicating the enhanced strut strength of the CNF-infused foams. During 30 min sonication time sample achieved the highest strength of  $1.12 \text{ kg/m}^2$  in the 3% foam.

### 3.3 Microstructure evolution



*Fig. 5. Scanning electron micrographs of (a) bare polyurethane and (b) polyurethane – CNF1 and (c) polyurethane –CNF3 foams.*

To enhance the significant of microstructures, we examined the SEM micrographs of the samples. The SEM micrographs of bare PU and CNF (1% and 3%) incorporated foams shown in Fig 5. The bare PU foam showed the porous and flexible morphology, CNF incorporated foams revealed the presence of CNF in the PU foam. It evidenced that the CNF incorporated without any signs of agglomeration in the PU matrix which can be due to the use of ultrasonication. With largely interconnected CNF channels and the width of the CNF frame was around  $121 \mu\text{m}$ . Moreover, the

CNF frame facilitated the electronic conductivity of the composite foams, and the junctions were connected in a pentagon patterns.

### 3.4 Surface chemical elements

The XPS data (C 1s spectrum) of the bare PU foam and the CNF (3%)-PU foam shown in Fig 6 (a). The C1 spectrum of the bare PU foam was used to understand the chemical composition of the base PU and a binding energy of 282 to 289 eV observed, suggesting the presence of C-H, C-C- and C-N groups.<sup>36</sup>

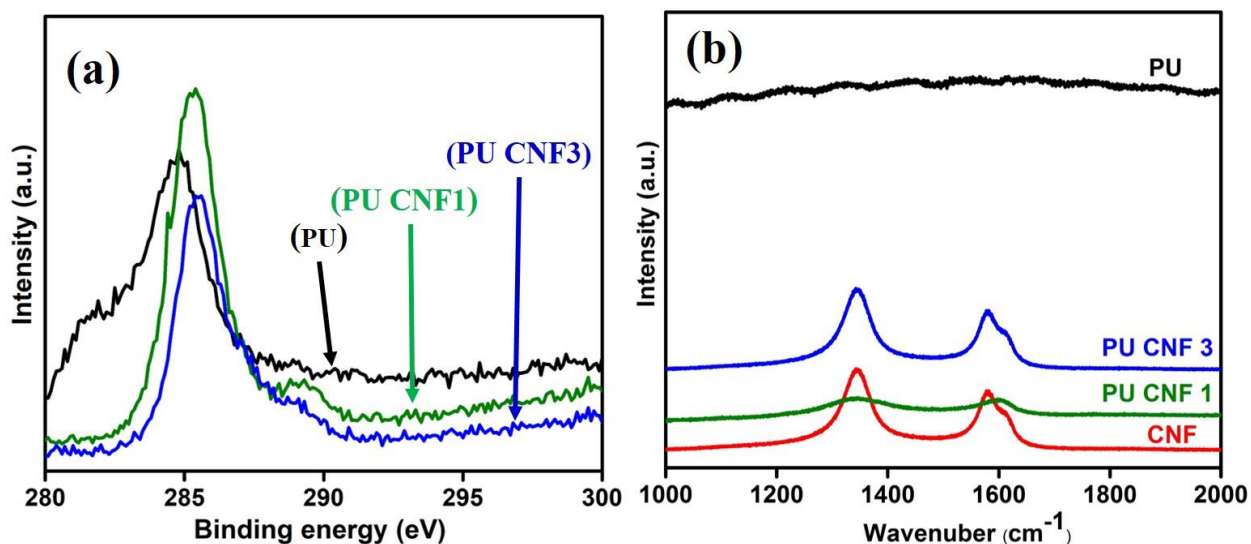


Fig. 6. PU/ PU CNF foams (a) X-ray photoelectron and (b) Raman Spectroscopy

The C1s spectrum of the CNF-PU foam showed a sharp band at 284.5 eV, which corresponds to the C-C counterparts, which can be mainly attributed to the CNFs blended uniformly in the PU matrix.<sup>37</sup> Since both PU and CNF are carbon materials, it is difficult to differentiate the state of elements via XPS analysis due to the limitation of the technique.

Hence, we used the Raman spectrum to understand the intermolecular bonding of the foams, as shown in Fig 6 (b). Raman spectroscopy is one of the most reliable techniques for understanding the crystallinity and the defect states in carbon materials, polymers and nanocomposite systems.<sup>38</sup>

The Raman spectrum of the PU bare foam showed the presence of the signature bands for amide

(III), isocyanate symmetric stretching, amide (II), amide (I) at 1325, 1450, 1545, and 1750  $\text{cm}^{-1}$  respectively. The observed Raman bands of the bare PU foam is in close agreement with previous reports of the Raman spectrum of polyurethane.<sup>39</sup> Furthermore, the Raman spectrum of the CNF-incorporated PU foams showed the presence of G and D bands observed in carbon materials. The G bands of CNF (1%) and CNF (3%) incorporated was observed at 1575 and 1579  $\text{cm}^{-1}$  respectively. Similarly, both the CNF-PU foams showed the presence of D band at 1350  $\text{cm}^{-1}$  that correspond to the presence of defect states in the CNF.<sup>40,41</sup> No bands were observed due to the bare PU in the CNF-PU foams. This is due to the lower vibration of organic stretching states in the PU as compared to that of the higher levels in CNFs.

### 3.5 Thermoelectric Properties

Thermopower is the thermoelectric voltage induced by the Seebeck effect in response to a temperature difference across the material. A high thermopower is one of the significant factors for the dynamic behavior of thermoelectric generators.

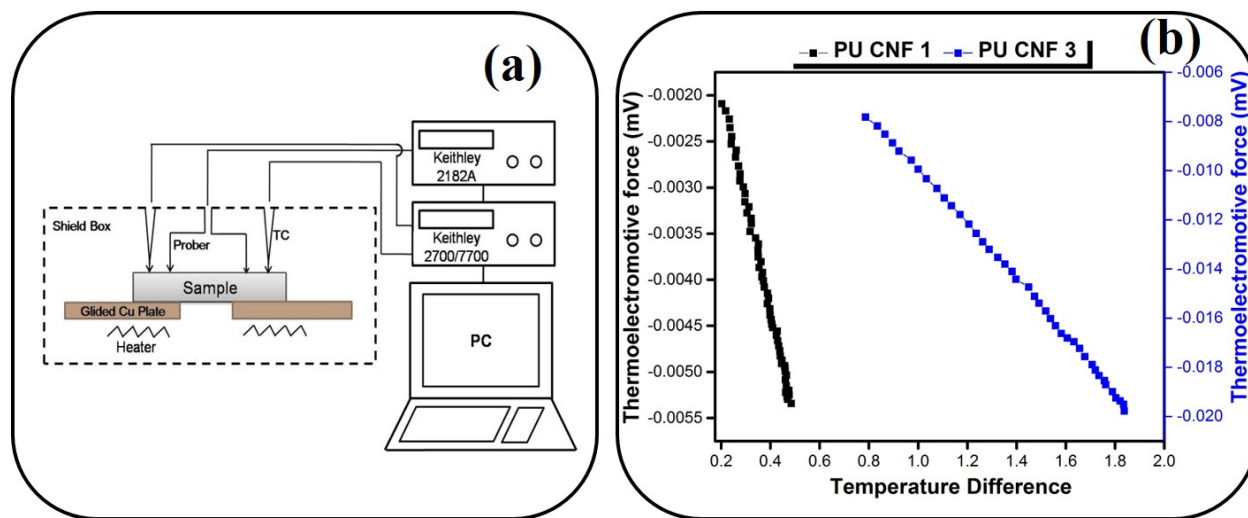


Fig. 7. (a) Experimental setup for Seebeck coefficient measurement and (b) TEMF of CNF incorporated PU foam as a function of temperature difference.

It is well known that polyurethane is an insulator so we cannot measure the Seebeck coefficient. Fig. 7 (b) shows the relation of the thermoelectromotive force of the CNF (1%) PU-foam and the CNF (3%) PU-foam, corresponding to the temperature difference. It can be seen that the Seebeck coefficient increases gradually from 1.2  $\mu\text{V/K}$  to 11.9  $\mu\text{V/K}$  as the CNF blend content increased from 1 % to 3 %. The high Seebeck coefficient is the average value calculated from the gradient in the relationship between the measured TEMF and the temperature difference. From this analysis, it is observed that a new novel foam material has been fabricated by incorporating carbon nanofibers in polyurethane with an enhanced Seebeck coefficient.

### **Conclusion:**

In this study, we investigated the effects of carbon nanofiber composites on the physical, structural and thermoelectric properties of Polyurethane foam materials. The carbon nanofiber provided good conductive pathways for the carriers in the composites, which resulted in a relatively high Seebeck coefficient. The Seebeck coefficient increased with increasing carbon nanofiber content, CNF (1%) PU-foam and CNF (3%)-PU foam is observed to have values of 1.2  $\mu\text{V/K}$  and 11.9  $\mu\text{V/K}$ , respectively.

### **References:**

1. H. Kim, Y. Miura, and C. W. Macoska, *Chem. Mater.* **2010**, 22, 3441.
2. P. Veluswamy, S. Suhasini, F. Khan, A. Gosh, M. Abhijit, Y. Hayakawa, and H. Ikeda, *Carbohydr. Polym.* **2016**, DOI : 10.1016/j.carbol.2016.11.065.
3. Q. Li, L. Chen, M. R. Gadinski, S. Zhang, G. Zhang, H. Li, a. Haque, L.-Q. Chen, T. Jackson, and Q. Wang, *Nat. Lett. Res.* **2015**, 523, 576.
4. A. L. Sharma, and A. T. Thakur, *J. Appl. Polym. Sci.* **2010**, 118, 2743.
5. P. Song, Z. Cao, Y. Cai, L. Zhao, Z. Fang, and S. Fu, *Polymer* **2011**, 52, 4001.

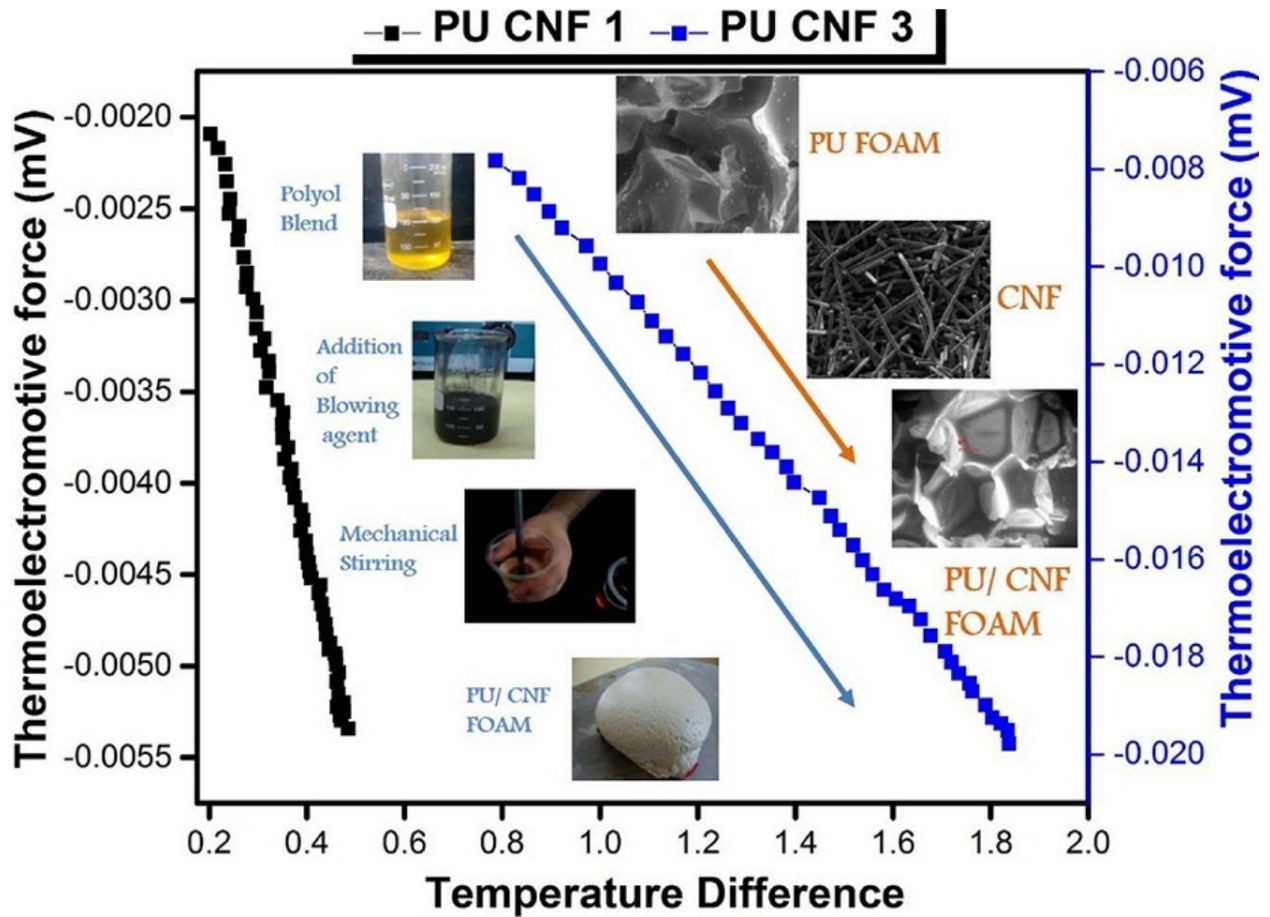
6. H. Gu, J. Guo, X. Yan, H. Wei, X. Zhang, J. Liu, Y. Huang, S. Wei, and Z. Guo, *Polymer* **2014**, 55, 4450.
7. Y. Fu, L. Liu, J. Zhang, and W. C. Hiscox, *Polymer* **2014**, 55, 6381.
8. D. R. Paul, and L. M. Robeson, *Polymer* **2008**, 49, 3187.
9. G. Z. Papageorgiou, Z. Terzopoulou, D. S. Achilias, D. N. Bikiaris, M. Kapnisti and D. Gournis, *Polymer* **2013**, 54, 4604.
10. K. Krishnamoorthy, S. Natarajan, S-J. Kim, and J. Kadarkaraithangam, *Mater. Express* **2011**,4, 329.
11. P. Veluswamy, S. Sathiyamoorthy, K. H. Chowdary, O. Muthusamy, K. Krishnamoorthy, T. Takeuchi, H. Ikeda, *J. Alloy Compd.* **2016**, DOI : 10.1016/j.jallcom.2016.10.196.
12. A. Kelarakis, S. Hayrapetyan, S. Ansari, J. Fang, L. Estevez, E. P. Giannelis, *Polymer*, **2010**, 51, 469.
13. Y. liu, and S. Kumar, *Acs Appl. Mater. Inter.* **2014**,6, 6069.
14. Y. Yang, Z-H. Lin, T. Hou, F. Zhang, and Z. L. Wang, *Nano Res.* **2012**, 12, 888.
15. Y. Zhang, W. Bai, X. Cheng, J. Ren, W. Weng, P. Chen, X. Fang, Z. Zhang, and H. Peng, *Angew. Chem. Int. Ed.* **2014**, 53, 14564.
16. Y. H. Jung, T-H. Chang, H. Zhang, C. Yao, Q. Zheng, V. W. Yang, *Nature Comm.* **2015**, 6 7170, 1.
17. C. Dun, C. A. Hewitt, H. Huang, D. S. Montgomery, J. Xu, and D. L. Carroll, *Phys. Chem. Chem. Phys.* **2015**, 17, 8591.
18. H. Anno, M. Hokazono, F. Akagi, M. Hojo and N. Toshima, *J. Electron Mater.* **2012**, 42, 1346.



19. M. Culebras, B. Uriol, C. Gomez, and A. Cantarero, *Phys. Chem. Chem. Phys.* **2015**, 17, 15140, p. 1.
20. J. Wang, K. Cai, H. Shen, and J. Yin, *Synt. Met.* **2014**, 195, 132.
21. M. Modesti, A. Lorenzetti, and S. Besco, *Polym. Eng. Sci.* **2007**, 1351.
22. G. M. Wu, Z. W. Kong, C. F. Chen, J. Chen, S. P. Huo, and J. C. Jiang, *J. Therm. Anal Calorim*, **2013**, 111, 735.
23. L. Yu, K. Dean, and L. Li, *Prog. Polym. Sci.* **2006**, 31, 576.
24. Z. Tang, M. M. Maroto-Valer, J. M. Andresan, J. W. Miller, M. L. Listemann, P. L. McDaniel, D. K. Morita, and W. R. Furlan, *Polymer* **2002**, 43, 6471.
25. M. Kotal, S. K. Srivastava, and B. Paramanik, *J. Phys. Chem. C* 2011, 115, 1496.
26. H. Lijuan, L. Fuwei, L. Ting, C. Feitai, and F. Pengfei, *J. Wuhan Univ. Natur. Sci.* **2012**, 17 5, 377.
27. T. Wida and C. W. Macosko, *J. Macromol. Sci. B* **2005**, 44, 897.
28. G. Mittal, V. Vivek, K. Y. Rhee, S-J. Park, and W. R. Lee, *J. Ind. Eng. Chem.* **2015**, 21, 11.
29. E. Ciecierska, M. Jurczyk-Kowalska, P. Bazarnek, M. Kowalski, S. Krauze, and M. Lewandowska, *J. Therm. Anal Calorim* **2015**, 1.
30. G. Harikrishnan, S. N. Singh, E. Kiesel, and C. W. Macosko, *Polymer* **2010**, 51, 3349.
31. C. Kimura, Y. Yamamuro, H. Aoki, and T. Sugino, *Diam. Relat. Mater.* **2007**, 16, 1383.
32. Y. Liu, C. Pan, and J. Wang, *J. Mater. Sci.* **2004**, 39, 1091.
33. M. C. Saha, Md. E. Kabir, and S. Jeelani, *Mater. Sci. Eng. A* **2008**, 479, 213.
34. A. K. Mishra, D. K. Chattopadhyay, B. Sreedhar, and K. V. S. N. Raju, *Prog. Org. Coat.* **2006**, 55, 231.

35. C. Kimura, Y. Yamamuro, H. Aoki, and T. Sugino, *Diam., Relat. Mater.* **2007**, 16, 1383.
36. E. Manikandana, G. Kavitha, and J. Kennedy, *Ceramic Int.* **2014**, 40, 16065.
37. H. Janik, B. Palys, and Z. S. Petrovic, *Macromol. Rapid Commun.* **2003**, 24, 265.
38. V. Pandiyarasan, J. Archana, A. Pavithra, V. Ashwin, M. Navaneethan, Y. Hayakawa, and H. Ikeda, *Mater. Lett.* **2016**, DOI : 10.1016/j.matlet.2016.11.047.
39. Y. Liu, C. Pan, and J. Wang, *J. Mater. Sci.* **2004**, 39, 1091.
40. L. Guadagno, M. Raimondo, V. Vittoria, L. Vertuccio, K. Lafdi, B. D. Vivo, P. Lamberti, G. Spinelli, and V. Tucci, *Nanotechnology*, **2013**, 24, 305704 (1-10).
41. K. Krishnamoorthy, K. Jeyasubramanian, M. Premanathan, G. Subbiah, H. S. Shin, and S. J. Kim, *Carbon* **2014**, 2, 328.
42. F. Salleh, Y. Suzuki, K. Miwa, and H. Ikeda, *Appl. Phys. Lett.* **2013**, 103 062107, 1.
43. F. Salleh, K. Miwa, and H. Ikeda, *J. Adv. Res. Phys.* **2012**, 3, 1.

Graphical abstract



Highlights

- A regeneration for waste heat recovery systems is proposed.
- Low cost, reliable, Multi application purpose.
- Vertical Measuring method is used to optimize thermal system.
- Power output and conversion efficiency increased by increasing CNF with PU FOAM.